

Non-Kramers doublets in PrNi₂Cd₂₀ and PrPd₂Cd₂₀

A. M. Konic,¹ R. B. Adhikari,¹ A. A. Kirmani,¹ A. Breindel,^{2,3}
R. Sheng,^{2,3} M. B. Maple,^{2,3} M. Dzero,¹ and C. C. Almasan¹

¹*Department of Physics, Kent State University, Kent, Ohio, 44242, USA*

²*Department of Physics, University of California at San Diego, La Jolla, CA 92093, USA*

³*Center for Advanced Nanoscience, University of California, San Diego, La Jolla, California 92093, USA*

(Dated: June 15, 2021)

Praseodymium-based 1-2-20 cage compounds PrT₂X₂₀ (*T* is generally Ti, V, Nb, Ru, Rh, Ir; and *X* is either Al, Zn or Cd) provide yet another platform to study non-trivial electronic states of matter ranging from topological and magnetic orders to unconventional multipolar orders and superconductivity. In this paper, we report measurements of the electronic heat capacity in two Pr-based 1-2-20 materials: PrNi₂Cd₂₀ and PrPd₂Cd₂₀. We find that the lowest energy multiplet of the Pr 4*f*² valence configuration is a Γ_3 non-Kramers doublet and the first excited states is magnetic Γ_4 triplet. By analyzing the dependence of the energy splitting between the ground and first excited singlet states on external magnetic field, we found that the maximum in the heat capacity corresponding to the Schottky anomaly in PrNi₂Cd₂₀, unlike PrPd₂Cd₂₀, shows pronounced linear dependence on external magnetic field. This effect is likely associated with the exchange interactions between the field-induced magnetic dipole moments.

PACS numbers: 71.10.Ay, 74.25.F-, 74.62.Bf, 75.20.Hr

I. INTRODUCTION

The discovery of the second-order mean-field-like phase transition in URu₂Si₂ provides a remarkable example of an ordered phase with an unknown order parameter, hence the name 'hidden-order transition'. Since its discovery almost thirty five years ago [1–4], quite significant experimental and theoretical progress has been made to get insights into the microscopic mechanism governing this transition (see Ref. 5 for the most recent review). In particular, two singlet states of the ground state valence configuration 5*f*² of the uranium ions seem to be a key feature to take into account in trying to identify the symmetry of the hidden order state [6, 7].

Naturally, one may wonder whether the 'hidden order' state could emerge in other materials with partially filled *f*-orbitals [8, 9]. Based on the body of knowledge accumulated for URu₂Si₂, the pre-requisite for the 'hidden-order' state seems to be that valence configuration of the *f*-orbital multiplet should have an even number of electrons (non-magnetic) and have a non-Kramers doublet as its ground state. At low enough temperatures, this allows one to represent the *f*-states on each ion in terms of two-level systems. Despite the fact that it is not possible to directly couple to the 'hidden-order' parameter, most likely a multipolar one, interactions between these two-level systems may then lead to either a 'hidden-order' or antiferromagnetic state, depending on the relative strength of the corresponding exchange parameter [7, 8].

Relatively novel 1-2-20 cage compounds with the chemical formula PrT₂X₂₀ (*T* is generally Ti, V, Nb, Ru, Rh, Ir; and *X* is either Al, Zn or Cd) [10–12] appear to satisfy these criteria. These materials are remarkable for a fairly strong hybridization between the conduction and *f*-electron states [13, 14]. Furthermore, at very low tem-

peratures some of these materials seem to develop some type of long-range order: PrIr₂Zn₂₀ and PrRh₂Zn₂₀ develop superconductivity at *T* ~ 0.05 and 0.6 K, respectively [10], PrTi₂Al₂₀ shows a ferroquadrupole order at 2 K [13, 15], PrRh₂Zn₂₀ an antiferroquadrupole order at 0.06 K, while the order is still undetermined in PrV₂Al₂₀ [8, 13, 16, 17].

The Pr ion in PrT₂X₂₀ (*X* = Zn, Al) finds itself in the 4*f*² (Pr³⁺) valence configuration with total angular momentum *J* = 4. The nine-fold degeneracy is lifted by the crystalline electric field resulting in a Γ_1 singlet, a non-Kramers Γ_3 doublet, and Γ_4 and Γ_5 triplet states also seen in similar Pr-based compounds [11, 12, 18]. Moreover, thermodynamic measurements seem to indicate that the lowest multiplet is a non-Kramers Γ_3 doublet [11, 19] which, as has already been noted above, opens the way for emergence of the exotic multipolar ordered phases [20, 21].

PrNi₂Cd₂₀ and PrPd₂Cd₂₀ are relatively new additions to the family of the 1-2-20 materials [12], which do not show any sign of ordering down to temperatures of *T* ~ 0.02 K. Also, it has recently been shown [22] that the ground state of the Pr ion in these materials is the non-Kramers Γ_3 doublet. In this context, we are motivated by not only confirming this recent finding by using heat capacity measurements, but also, based on the heat capacity data, to estimate the position of the first excited triplet as well as the strength of the exchange interactions in these compounds, hence, to predict what state - superconductivity or some kind of multipolar order - these materials would develop first upon further cooling into the millikelvin range.

In this paper, we report specific heat measurements done on single crystalline samples of PrNi₂Cd₂₀ and PrPd₂Cd₂₀ in external magnetic fields. Fits of the specific heat data at temperatures below 4 K, and entropy

calculations from those fits were done to further investigate the ground states of these systems. We found that the ground state of Pr ion is, indeed, the non-Kramers Γ_3 doublet. Furthermore, the predominantly linear dependence of the peak in the heat capacity on external magnetic field in $\text{PrNi}_2\text{Cd}_{20}$ suggests that, on one hand, the energy between the ground state doublet and first excited triplet state is small enough for the triplet state to be completely excluded from the analysis and, on the other hand, the interaction between the induced dipole moments lead to boosting the linear-in-field contribution.

II. EXPERIMENTAL DETAILS

Single crystals of $\text{PrNi}_2\text{Cd}_{20}$ and $\text{PrPd}_2\text{Cd}_{20}$ were grown at the University of California San Diego using the Cd self-flux technique described in Refs. [12, 23]. Analysis of the powder x-ray diffraction (XRD) patterns obtained via a Bruker D8 Discover x-ray diffractometer was done to determine the crystal structure and quality of the single crystals [12]. This analysis showed both samples to be single phase crystals lacking any indication of impurity phases [12]. The structure for both samples was determined to be the $\text{CeCr}_2\text{Al}_{20}$ -type cubic structure, having a space group of $Fd\bar{3}m$ [12, 23].

We performed heat capacity measurements on a $\text{PrNi}_2\text{Cd}_{20}$ sample with a mass of 0.9 mg and a $\text{PrPd}_2\text{Cd}_{20}$ sample with a mass of 1.1 mg, using the He-3 insert for a Quantum Design Physical Property Measurement System (PPMS) employing a standard thermal relaxation technique. For better thermal contact between the samples and measurement platform, the contact surface of each sample was polished with sand paper. These measurements were performed in magnetic fields H ranging from 0 to 14 T applied along the c -axis, i.e., perpendicular to the single crystals and over a temperature range of $0.39 \text{ K} \leq T \leq 50 \text{ K}$.

III. RESULTS AND DISCUSSION

Figure 1 depicts the temperature dependence of the measured specific heat normalized by temperature C/T for single crystalline samples of $\text{PrNi}_2\text{Cd}_{20}$ and $\text{PrPd}_2\text{Cd}_{20}$ obtained in zero magnetic field. As can be seen, both compounds exhibit a clear Schottky-type peak just below 5 K, with additional upturns seen below 1 K. To further investigate these features of the specific heat, we examined the $4f$ electrons contribution to the specific heat in more detail.

In order to extract the $4f$ electrons contribution to the specific heat, we subtracted the specific heat of the non-magnetic analog compound $\text{LaNi}_2\text{Cd}_{20}$ (data also shown in Fig. 1) from the specific heat of $\text{PrNi}_2\text{Cd}_{20}$ and $\text{PrPd}_2\text{Cd}_{20}$. This graphical subtraction of the non-magnetic analog compound over the whole T range, rather than a fit of the high T data assuming that the

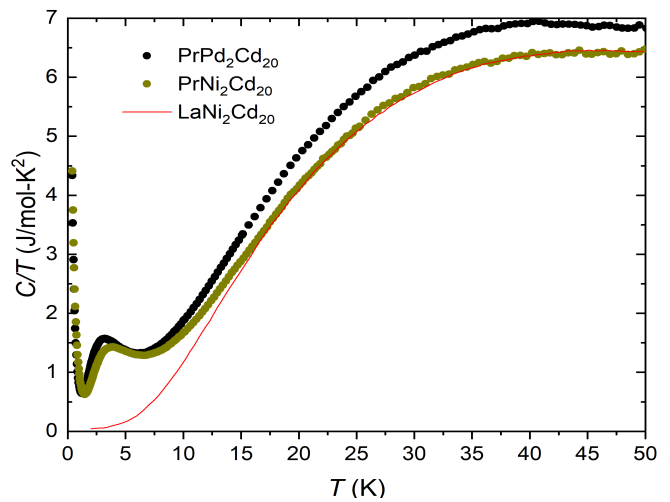


FIG. 1: Temperature dependence of specific heat normalized by temperature, C/T , for both $\text{PrNi}_2\text{Cd}_{20}$ and $\text{PrPd}_2\text{Cd}_{20}$. The non-magnetic compound $\text{LaNi}_2\text{Cd}_{20}$ was used to subtract the phonon contribution to the specific heat to further analyze the $4-f$ electron contribution.

phonon contribution to the specific heat dominates, gives an accurate depiction of the $4f$ contribution to the specific heat [24]. Due to the overlap between the data for $\text{PrNi}_2\text{Cd}_{20}$ and $\text{LaNi}_2\text{Cd}_{20}$ in the higher temperature range, where the phonon contribution to specific heat dominates, the $\text{LaNi}_2\text{Cd}_{20}$ data can be subtracted from the $\text{PrNi}_2\text{Cd}_{20}$ data directly. Given that we did not have specific heat data available for the non-magnetic analog of $\text{PrPd}_2\text{Cd}_{20}$, we utilized the fact that in the higher temperature range, where the lattice (i.e., phonon) contribution dominates, the slopes of C/T vs T for $\text{PrPd}_2\text{Cd}_{20}$ and $\text{LaNi}_2\text{Cd}_{20}$ are very similar. As a result, we scaled the C/T data of $\text{PrPd}_2\text{Cd}_{20}$ and $\text{LaNi}_2\text{Cd}_{20}$ with a scaling factor of 1.085, and then subtracted the $\text{LaNi}_2\text{Cd}_{20}$ data from the $\text{PrPd}_2\text{Cd}_{20}$ data. The 1.085 scaling factor reflects the small difference between the Debye temperatures of $\text{LaNi}_2\text{Cd}_{20}$ and $\text{PrPd}_2\text{Cd}_{20}$.

By subtracting the specific heat of the non-magnetic reference compound from the measured specific heat, we obtained the electronic and magnetic contributions to the specific heat. Then, to obtain the electronic contribution to the specific heat, we have also subtracted the nuclear contribution to the specific heat.

Next, we determined the energy level splitting and the entropy to further study the ground state structure of the $4f$ multiplet, as presented below. Figures 2(a) and 2(b) and their insets depict, for both compounds, the temperature dependencies of C_{el}/T on the left axis and of the entropy S on the right axis. We fitted the peaks near 4 K (data and fits shown in the insets of the two figures), and the upturns below 1 K (data and fits shown in the main panel of the figures) using a two-level Schottky model

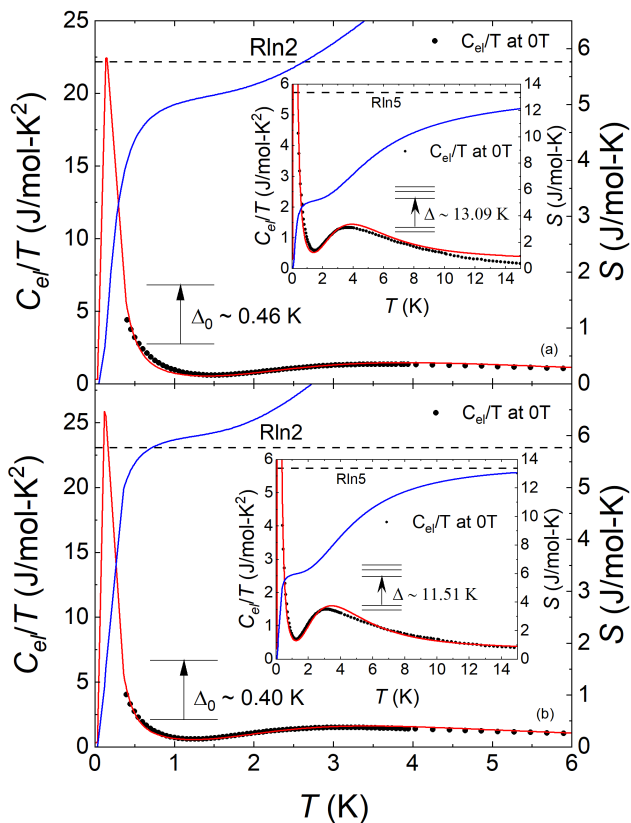


FIG. 2: Electron specific heat normalized by temperature, C_{el}/T , (left axis) and entropy S (right axis) as a function of temperature T for (a) PrNi₂Cd₂₀ and (b) PrPd₂Cd₂₀. The main panels focus on the low T upturns, while the insets reveal the Schottky-type peaks at higher T . Fits of the Schottky-type peaks (red lines) in both the main panels and insets were done using a two-level model (see text for details).

given by [12]:

$$\frac{C_{el}}{T} = \gamma + \frac{A\Delta^2 g_a g_b e^{-\Delta/T}}{T^3 (g_a + g_b e^{-\Delta/T})^2}. \quad (1)$$

Here γ is the Sommerfeld coefficient, $A \leq 1$ is a phenomenological parameter which reflects the degree of the hybridization between Pr ions and the conduction band, Δ is the energy level splitting, and g_a and g_b are the degeneracy of the ground and first excited state, respectively. In what follows, we use γ , A , and Δ as fitting parameters.

By fitting the Schottky peaks present in the two insets of Figs. 2(a) and 2(b), we obtain values for the energy splitting between the ground state and first excited state. We obtained the best fits with $g_a = 2$ and $g_b = 3$. This implies that the ground state is a non-Kramers doublet and the first excited state is a triplet. We obtained $\Delta = 13.09$ K, with $A = 1$ for PrNi₂Cd₂₀ and $\Delta = 11.51$ K, with $A = 1$ for PrPd₂Cd₂₀, which are in good agreement with values reported previously [12]. The fact that in both of these systems $A = 1$ implies the absence of

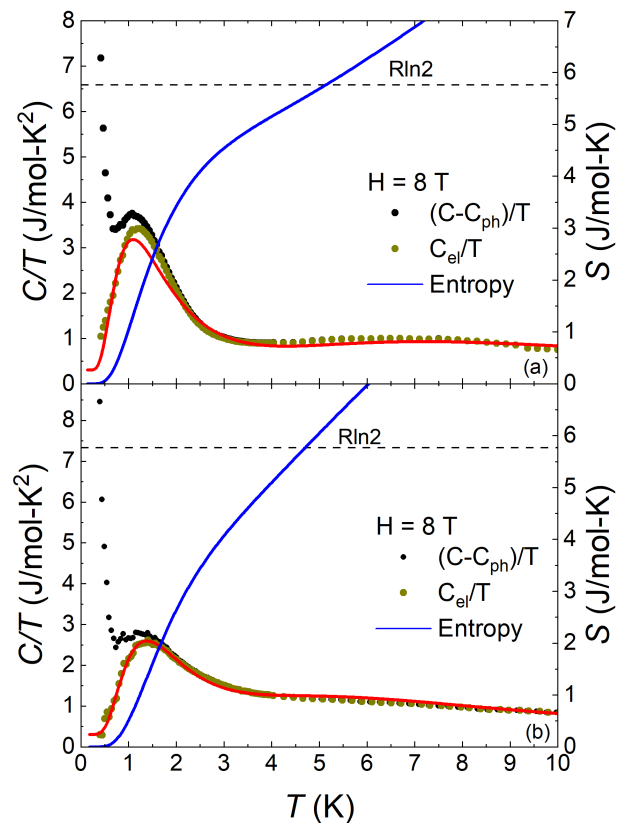


FIG. 3: Specific heat normalized by temperature, $(C - C_{ph})/T$, (left axis) and entropy S (right axis) vs temperature T data measured in an applied magnetic field H of 8 T for (a) PrNi₂Cd₂₀ and (b) PrPd₂Cd₂₀. The Schottky peaks seen just above 1 K is a result of the shift in the peak location from $T < 0.3$ K, in response to the 8 T field. Note that the entropy exceeds the $R \ln 2$ value signalling the field-induced admixture of the first excited triplet.

hybridization between Pr ions and the conduction band. This is consistent with the non-Kramers doublet nature of the ground state multiplet.

Next, we assume that the Schottky upturns in specific heat seen below 1 K (main panel of Figs. 2(a-b)) for each compound is a result of the lifting of the degeneracy of the non-Kramers doublet ground state. Hence, we fitted these data with Eq. (1) with $g_a = g_b = 1$ and obtained values for the energy splitting between the two levels of the ground state to be, $\Delta_0 = 0.46$ K and $\Delta_0 = 0.40$ K for PrNi₂Cd₂₀ and PrPd₂Cd₂₀, respectively. We note that we obtained worse fits of these data by choosing other values of g_a and g_b , hence other ground state options. These results, therefore, further confirm that the ground state of both compounds is the non-Kramers doublet.

In order to further check the validity of the conclusions we have drawn from our fits in Figs. 2(a) and 2(b) and their insets, we also calculated the entropy from the fits

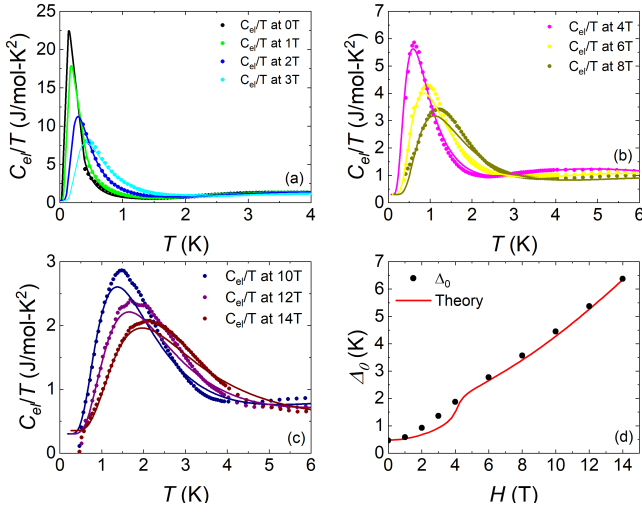


FIG. 4: (a-c) Electronic specific heat normalized by temperature C_{el}/T vs temperature T and Schottky fits (solid lines) in applied magnetic fields H for PrNi₂Cd₂₀. (d) Energy gap (Δ_0) between the two ground state levels, as a function of applied magnetic field H .

of the Schottky contribution to the specific heat as

$$S(T) = \int_0^T [C_{el}(T) - \gamma T] \frac{dT}{T}, \quad (2)$$

see blue lines in Figs. 2. As the main panels of Figs. 2(a) and 2(b) reveal, the entropy of the Schottky peak below 1 K due to the splitting of the ground state reaches the full $R \ln 2 = 5.76$ J/mol K near 2.62 K for PrNi₂Cd₂₀ and 0.71 K for PrPd₂Cd₂₀. Therefore, this result provides further confirmation that the Γ_3 non-Kramers doublet is the ground state multiplet of both compounds studied here.

In addition, we note that the higher energy multiplets, specifically the triplet state above the ground state doublet, becomes accessible as the temperature increases. As with the lower temperature Schottky peak, we expect the overall change in entropy after this multiplet is accessed to be equal to $R \ln(g_a + g_b)$, where now $g_a = 2$, and $g_b = 3$. Thus, we expect a change in entropy equal to $R \ln 5 = 13.4$ J/mol K. As can be seen in the insets of Figs. 2(a) and 2(b), we obtained 90.5% of the expected value, i.e., $S = 12.13$ J/mol K for PrNi₂Cd₂₀ at $T = 15$ K and 97.7%, $S = 13.09$ J/mol K for PrPd₂Cd₂₀ at $T = 15$ K. Thus, we find that in this temperature range the contribution to the entropy comes from the non-Kramers doublet along with the two lowest lying states in the first excited triplet.

In Figures 3(a) and 3(b) we show the specific heat for both compounds measured in an applied magnetic field of 8 T. These plots exhibit how C_{el} (dark yellow data points) was obtained by subtracting a low T nuclear contribution from $(C - C_{ph})$ (black data points), and was used to obtain the data for fitting in the other magnetic

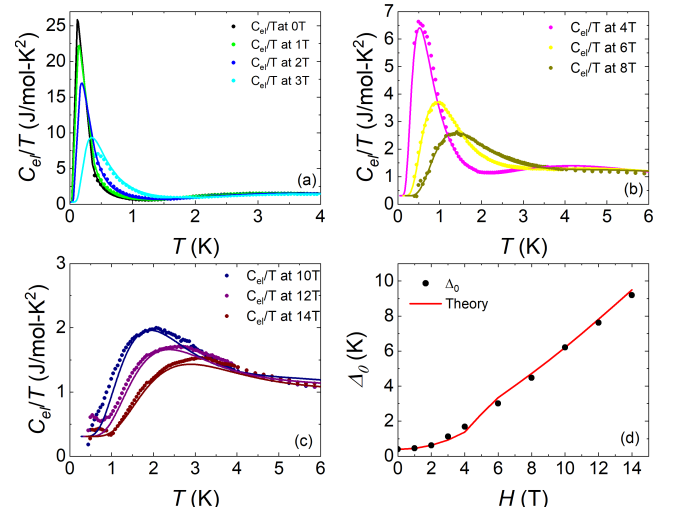


FIG. 5: (a-c) Electronic specific heat normalized by temperature C_{el}/T vs temperature T and Schottky fits (solid lines) in applied magnetic fields H for PrPd₂Cd₂₀. (d) Energy gap (Δ_0) between the two ground state levels, as a function of applied magnetic field H .

fields measured as well. These results reveal that the zero-field upturns seen in Figs. 2(a) and 2(b) below 1 K shift to higher temperatures with increasing applied magnetic field and the peaks that are not visible in $H = 0$ down to 0.3 K become visible at $T \approx 1$ K in a magnetic field $H = 8$ T. Fits of these Schottky peaks with Eq. (1) with $g_a = g_b = 1$ are shown on the figures in red. At this magnetic field we obtained $\Delta_0 = 3.57$ K for PrNi₂Cd₂₀ and $\Delta_0 = 4.48$ for PrPd₂Cd₂₀.

Figures 3(a) and 3(b) also show the entropy (plotted on the right axes, blue lines) calculated from the fits of the Schottky peak in 8 T for the two compounds using Eq. (2). Here, both compounds achieve the expected $R \ln 2 = 5.76$ J/mol·K at $T \approx 5$ K. This confirms that, indeed, the Schottky peak observed in 8 T for both compounds is a result of the splitting of the ground-state Γ_3 non-Kramers doublet. An entropy larger than $R \ln 2$ at $T > 5$ K is a result of the excited triplet states contributing at the higher temperatures.

We plot the temperature dependence of C_{el}/T data for PrNi₂Cd₂₀ and PrPd₂Cd₂₀ measured in applied magnetic fields from 0 to 14 T in Figs. 4 and 5, respectively. We note that, even though the ground state valence configuration of the Pr ions is non-magnetic, the location of the peaks exhibit a dependence on magnetic field. This dependence for both materials can be understood using a simple model of interacting two-level systems in an external magnetic field, which we discuss in the theoretical model section below.

By fitting the specific heat data of Figs. 4 and 5 with Eq. (1) where $g_a = g_b = 1$, we extract the values of the energy splitting Δ_0 between the two levels of the non-Kramers doublet ground state as a function of magnetic field for the two compounds. We show these results in

Figs. 4(d) and 5(d). The red solid lines are fits of these data using a phenomenological model, as discussed in the next section.

IV. PHENOMENOLOGICAL MODEL AND DISCUSSION

In order to fit the experimental data for the dependence of the energy splitting on external magnetic field seen in the insets of Fig. 4, we consider the ground state non-Kramers doublet with state vectors

$$\begin{aligned} |\Gamma_3, a\rangle &= \sqrt{\frac{7}{24}} (|4\rangle + |-4\rangle) - \sqrt{\frac{5}{12}} |0\rangle, \\ |\Gamma_3, b\rangle &= \frac{1}{\sqrt{2}} (|2\rangle + |-2\rangle). \end{aligned} \quad (3)$$

Our data indicate that there is a small energy splitting Δ_0 between $|\Gamma_3, a\rangle$ and $|\Gamma_3, b\rangle$ states. For the first excited triplet state we use the results of Ref. 12 and assume that it is described by the Γ_5 triplet which lies at the energy Δ above Γ_3 :

$$\begin{aligned} |\Gamma_5, a(b)\rangle &= \sqrt{\frac{7}{8}} |\pm 3\rangle - \sqrt{\frac{1}{8}} |\mp 1\rangle, \\ |\Gamma_5, c\rangle &= \frac{1}{\sqrt{2}} (|2\rangle - |-2\rangle). \end{aligned} \quad (4)$$

Given that in our experiments the magnetic field is along the c -axis, $\vec{H} \parallel [001]$, one can immediately check that it will induce virtual transitions between $|\Gamma_3, b\rangle$ and $|\Gamma_5, c\rangle$ states. Assuming that magnetic field $H < \Delta/\mu_B$, these virtual transitions lead to decrease in the energy of the $|\Gamma_3, a\rangle$ state by $\delta\varepsilon \approx (\mu_B H)^2/\Delta$, while the energy of the $|\Gamma_5, c\rangle$ state increases by the same amount. Furthermore, the energy of the $|\Gamma_5, a\rangle$ decreases linearly with increasing magnetic field.

With these provisions, we fit the dependence of the peak in the heat capacity on the magnetic field at low temperatures using a model with three energy levels ε_1 , ε_2 and ε_3 . The first two energy levels correspond to the non-Kramers doublet states: $\varepsilon_1 = -\Delta_0/2 - \gamma \left[\sqrt{\Delta^2 + (\mu_B H)^2} - \Delta \right]$ and $\varepsilon_2 = +\Delta_0/2$. The third energy level corresponds to $|\Gamma_5, a\rangle$ state, $\varepsilon_3 = \Delta - \alpha\mu_B H$. We consider α and γ as the fitting parameters. The best fits for the experimental data shown in insets of Fig. 4 were obtained for $\Delta_0/2 \approx 0.495\text{K}$ and $\gamma \approx 2.95$. The values of the remaining parameters Δ and α are: $\Delta = 10\text{K}$, $\alpha = 0.1$ for $\text{PrPd}_2\text{Cd}_{20}$ and $\Delta = 12\text{K}$, $\alpha = 1.15$ for $\text{PrNi}_2\text{Cd}_{20}$. Note that the values for both Δ_0 and Δ , which we have chosen independently for the fits, are in agreement with those extracted from the heat capacity. Significantly higher values of the parameter α in $\text{PrNi}_2\text{Cd}_{20}$ are likely due to enhanced dipole-dipole interactions in this material.

Lastly, we note that in principle the very similar results could be found under the assumption of Γ_4 being the first

excited triplet. In order to verify that our assumption of Γ_5 being the first excited triplet indeed holds, more detailed studies of the dependence of the Schottky peak on various directions of the external magnetic field will have to be carried out.

V. CONCLUDING REMARKS

We performed specific heat measurements of $\text{PrNi}_2\text{Cd}_{20}$ and $\text{PrPd}_2\text{Cd}_{20}$ in magnetic fields ranging from 0 to 14 T and in temperatures ranging from 50 K down to 0.39 K. Schottky fits of the specific heat curves show that in both compounds studied the ground state is the non-Kramers Γ_3 doublet, while the first excited state is a triplet. Entropy calculations provide further evidence. Through Schottky fits of the specific heat curves we also extracted the values of the energy level splitting between the two singlets that make up the doublet ground state and between the doubly-degenerate ground state and the triply-degenerate first-excited state. We also obtained the magnetic field dependence of the energy level splitting of the ground state. An analysis of this H dependence of the energy splitting of the ground state shows that the exchange interactions between the two-level systems are weak in $\text{PrNi}_2\text{Cd}_{20}$, but they cannot be neglected in $\text{PrPd}_2\text{Cd}_{20}$. These latter results, therefore, suggest that in the millikelvin range of temperatures $\text{PrPd}_2\text{Cd}_{20}$ could develop superconductivity, while $\text{PrNi}_2\text{Cd}_{20}$ will develop long-range order that could be either multipolar or magnetic.

VI. ACKNOWLEDGMENTS

The work at Kent State University was supported by the National Science Foundation grants DMR-1904315, DMR-BSF-2002795, and by the U.S. Department of Energy, Office of Science, Office of Basic Energy Sciences under Award No. DE-SC0016481. The work at UCSD was supported by the US Department of Energy, Office of Basic Energy Sciences, Division of Materials Sciences and Engineering, under Grant No. DE-FG02-04ER45105 (single crystal growth) and the National Science Foundation under Grant No. DMR-1810310 (materials characterization).

-
- [1] T. T. M. Palstra, A. A. Menovsky, J. v. d. Berg, A. J. Dirkmaat, P. H. Kes, G. J. Nieuwenhuys, and J. A. Mydosh, *Phys. Rev. Lett.* **55**, 2727 (1985).
- [2] M. B. Maple, J. W. Chen, Y. Dalichaouch, T. Kohara, C. Rossel, M. S. Torikachvili, M. W. McElfresh, and J. D. Thompson, *Physical Review Letters* **56**, 185 (1986).
- [3] W. Schlabitz, J. Baumann, B. Pollit, U. Rauchschwalbe, H. M. Mayer, U. Ahlheim, and C. D. Bredl, in *Ten Years of Superconductivity: 1980–1990* (Springer Netherlands, 1986), pp. 89–95.
- [4] J. A. Mydosh, *Philosophical Magazine* **94**, 3640 (2014).
- [5] J. A. Mydosh, P. M. Oppeneer, and P. S. Riseborough, *Journal of Physics: Condensed Matter* **32**, 143002 (2020).
- [6] K. Haule and G. Kotliar, *Nature Physics* **5**, 796 EP (2009).
- [7] K. Haule and G. Kotliar, *EPL (Europhysics Letters)* **89**, 57006 (2010).
- [8] A. S. Patri, A. Sakai, S. Lee, A. Paramekanti, S. Nakatsuji, and Y. B. Kim, *Nature Communications* **10**, 4092 (2019).
- [9] S. Lee, S. Trebst, Y. B. Kim, and A. Paramekanti, *Phys. Rev. B* **98**, 134447 (2018).
- [10] T. Onimaru, K. T. Matsumoto, Y. F. Inoue, K. Umeo, Y. Saiga, Y. Matsushita, R. Tamura, K. Nishimoto, I. Ishii, T. Suzuki, et al., *Journal of the Physical Society of Japan* **79**, 033704 (2010).
- [11] T. Onimaru, N. Nagasawa, K. T. Matsumoto, K. Wakiya, K. Umeo, S. Kittaka, T. Sakakibara, Y. Matsushita, and T. Takabatake, *Physical Review B* **86** (2012).
- [12] D. Yazici, T. Yanagisawa, B. D. White, and M. B. Maple, *Physical Review B* **91**, 115136 (2015).
- [13] A. Sakai and S. Nakatsuji, *Journal of the Physical Society of Japan* **80**, 063701 (2011).
- [14] Y. Tokunaga, H. Sakai, S. Kambe, A. Sakai, S. Nakatsuji, and H. Harima, *Phys. Rev. B* **88**, 085124 (2013).
- [15] T. Onimaru, K. T. Matsumoto, Y. F. Inoue, K. Umeo, T. Sakakibara, Y. Karaki, M. Kubota, and T. Takabatake, *Phys. Rev. Lett.* **106**, 177001 (2011).
- [16] T. Onimaru, N. Nagasawa, K. T. Matsumoto, K. Wakiya, K. Umeo, S. Kittaka, T. Sakakibara, Y. Matsushita, and T. Takabatake, *Phys. Rev. B* **86**, 184426 (2012).
- [17] F. Freyer, J. Attig, S. Lee, A. Paramekanti, S. Trebst, and Y. B. Kim, *Phys. Rev. B* **97**, 115111 (2018).
- [18] H. Kusunose, *Journal of the Physical Society of Japan* **85**, 064708 (2016).
- [19] B. D. White, J. D. Thompson, and M. B. Maple, *Physica C: Superconductivity and its Applications* **514**, 246 (2015), *superconducting Materials: Conventional, Unconventional and Undetermined*.
- [20] G. Zhang, J. S. Van Dyke, and R. Flint, *Phys. Rev. B* **98**, 235143 (2018).
- [21] J. S. Van Dyke, G. Zhang, and R. Flint, *Phys. Rev. B* **100**, 205122 (2019).
- [22] T. Yanagisawa, H. Hidaka, H. Amitsuka, S. Nakamura, S. Awaji, E. L. Green, S. Zherlitsyn, J. Wosnitza, D. Yazici, B. D. White, et al., *Philosophical Magazine* pp. 1–14 (2020).
- [23] V. W. Burnett, D. Yazici, B. D. White, N. R. Dilley, A. J. Friedman, B. Brandom, and M. B. Maple, *Journal of Solid State Chemistry* **215**, 114 (2014).
- [24] J. A. Morrison and D. M. T. Newsham, *Journal of Physics C: Solid State Physics* **1**, 370 (1968).